Investigation of oscillating behaviour of a Koch fractal drum

Jonas Gran Melandsør

I. DISCLAIMER

This work is one part of the exam in TFY4235 computational physics at NTNU. Therefore this report does not have all the requirements of an article. The report is shared to help explain the code also available at in the Git repository.

II. INTRODUCTION

A. The Hemholtz equation

$$-\nabla^2 U(\mathbf{r},\omega) = \frac{\omega^2}{c^2} U(\mathbf{r},\omega), \quad \text{in } D, \tag{1a}$$

$$U(\mathbf{r},\omega) = 0 \quad \text{on } \partial D, \tag{1b}$$

where U is the displacement, ω the angular frequency, c the speed of sound of the media, D is the region inside the fractal drum and ∂D is the boundary. Further, Equation 1b is a Dirichlet boundary meaning that the boundary cannot be displaced as it is bounded. The eigenvalues of Equation 1a are $\frac{\omega^2}{c^2}$ eigenvalues of the system, where ω is the eigenfrequency, wiht the eigenmode $U(\mathbf{r},\omega)$[1].

B. Biharmonic equation

If one instead is interested in the vibration eigenfrequencies and modes of the of a clamped thin plate, rather than for a vibrating membrane, one can further constrain the displacement mode of the the boundary. For a region inside a clamped thin plate fractal plate Ω the displacement W can be defined as

$$\nabla^4 W(\mathbf{x},\omega) = \lambda W(\mathbf{x},\omega) \quad \text{in } \Omega, \tag{2a}$$

$$W(\mathbf{x},\omega) = 0 \quad \text{on } \partial\Omega, \tag{2b}$$

$$\partial_n W(\mathbf{x},\omega) = 0 \quad \text{on } \partial\Omega, \tag{2c}$$

where $\nabla^4 = \nabla^2\nabla^2$ and $\partial_n = \hat{\mathbf{n}} \cdot \nabla$ is the outward pointing derivative.

III. MODELS AND METHODS

All the coding was performed in a Jupyter notebook with Julia kernel.

To generate the fractal it was made use of that the Koch fractal splits each line segments into four and adds square wave shape around it. Each time the orientation changes, which was done be rotating the square wave using the first point as a pivot. The rotation depends on the orientation of the line segment, which was implemented by checking the start and endpoint of the line segment.

A. Point classification

To generate a lattice, it was used that the grid constant, distance between lattice points, was $\delta_l = \frac{L}{4^l}$[1]. To make a lattice that dynamically updates to contains the fractal based on the fractal level l, the lenght must be $L_l = L + 2\sum_{n=1}^{l} \delta_n$ with L the width of the lattice and δ_n the grid constant.

One of the methods implemented for for determining the lattice points inside the fractal drum was the based on the winding number as described in[2]. The pseudo code is given in algorithm 1. The other method to classify data points that was used was based on the LibGEOS library in Julia. This library contained a function called *within()* that calculated points inside a polygon.

Algorithm 1 Winding number classifier

Require: M : lattice matrix, fractal
Ensure: Lattice points inside fractal are classified as 1.

```
L ← size(M, 1)
C ← fill(−1, size = L^2)                    ▷ Assume all points outside
f ← {}                                      ▷ Initialize empty set
for j in 1 : L do
    for i in 1 : L do
        p ← M[i, j]                         ▷ Lattice point
        θ ← 0                               ▷ Angle
        if p ∈ f then continue              ▷ Fractal points are not classified
        end if
        for k in lenght(fracal)-1 do
            a ← fractal[k] − p              ▷ Dist(p, a fractal point)
            b ← fractal[k + 1] − p          ▷ Dist(p, next fractal point)
            θ ← θ + arctan((a_x b_y − a_y b_x) / (a · b))
        end for
        if |θ| > 1e − 5 then                ▷ Threshold to tackle precision error
            C[i, j] = 1                     ▷ Points inside set to 1
        end if
    end for
end for
```

When generate the finite differences matrix for the Hemholtz equations, it was beneficial to label the points inside the fractal with a unique ID. The labeling was done by iterating through each of the points where coefficient matrix was non-zero, and labeling them by increasing integers. The result is seen in Figure 3, where the interior points are labeled from top left downwards and rightwards. The fractal are added on on top giving a value of zero at the boundary, and therefore fullfil Equation 1b.

B. Finite differences

Taking only the nearest neighbors into account a five point stencil, using central differences, Equation 3 is obtained as a

discretization of Equation 1a

$$-\frac{1}{(h)^2}[U_{m+1,n}+U_{m-1,n}+U_{m,n+1}+U_{m,n-1}-4U_{m,n}]=\frac{\omega^2}{c^2}U_{mn}, \tag{3}$$

where $h=\delta_l$ and m,n. Central differences are of order $O(h^2)$[3], making the discretization of Equation 3 of second order. By also adding the next nearest neighbors To improve the order, the nine points stencil was also used

$$\begin{aligned}\frac{\omega^2}{c^2}U_{mn}=\frac{1}{12h^2}[&U_{m+2,n}-16U_{m+1,n}-16U_{m-1,n}\\&+U_{m-2,n}+60U_{m,n}+U_{m,n+2}\\&-16U_{m,n+1}-16U_{m,n-1}+U_{m,n-2}],\end{aligned} \tag{4}$$

which is of order four[3].
Equation 2a can be discretized using a 13 point stencil:

$$\begin{aligned}\lambda W_{mn}=\frac{1}{h^4}[&W_{m+2,n}-8W_{m+1,n}-8W_{m-1,n}\\&+W_{m-2,n}+2W_{m+1,n+1}+2W_{m+1,n-1}\\&+16W_{m,n}+2W_{m-1,n-1}+2W_{m-1,n+1}\\&+W_{m,n+2}-8W_{m,n+1}-8W_{m,n-1}+W_{m,n-2}].\end{aligned} \tag{5}$$

The 13 point stencil is of order $O(h^2)$[3]. To address Equation 2c, one can write Equation 2c using finite difference. As the points outside the lattice are fixed, the finite difference scheme must be the backward difference $\partial_n W=\frac{W_{i,j}-W_{i-1,j}}{h}$ to order $O(h)$. Since $W_{i,j}=0$ are from by Equation 2b, $W_{i-1,j}=0$ for Equation 2c to be fulfilled. Therefore all neighboring points to the fractal that are within the fractal are set to zero. Therefore the area that can vibrate are smaller for the thin clamped plate than for the fractal drum.

each of the points in the fractal and setting the neighbor to zero if the neighbor also is inside the fractal.

C. Solving the system

Equation 3, Equation 5 and Equation **??** can be implemented as a coefficient matrix, A. Each of the factors in front of $U_{i,j}$ is the value assigned to the correct index A, a mapping performed by using the coefficient matrix C_{mn} and its neighbors as indexes of the A, e.g. $A[C_{mn},C_{m-1,n}]=-\frac{1}{h^2}$ for the five points stencil.

Having the coefficient matrix, the eigenvalues and eigenmodes can be found be using a direct solver. Since the matrices get quite large for $l\geq 3$ and far from all of the matrix element are non-zero, the sparse matrices and solver from the library ARPACK was used.

IV. RESULTS

The ten smallest eigenmodes for the five point stencil solution is plotted in Figure 4, Figure 5 and Figure 6. The eigenfrequencies are shown in Table I. The eigenfrequencies for the forth order Hemholtz are shown in Table II.

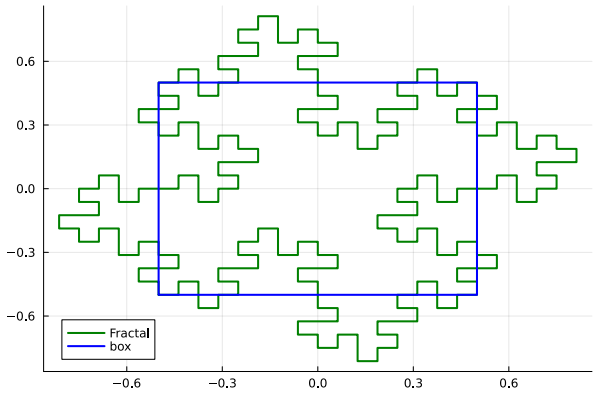

(a) $l=2$

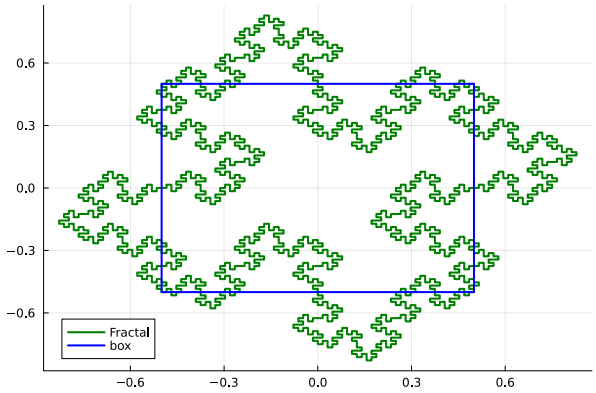

(b) $l=3$

FIG. 1: Koch fractal for different fractal level l

TABLE I: Eigenvalues and related quantities using a second-order finite difference stencil.

mode_index	eigenvalue	degeneracy	ratio
0	9.42994	1	2.12248
1	14.1469	2	3.18417
2	14.1469	2	3.18417
3	14.4199	1	3.24562
4	14.4969	1	3.26294
5	15.0824	2	3.39473
6	15.0824	2	3.39473
7	17.6559	1	3.97397
8	18.9114	1	4.25655
9	19.4563	2	4.37921

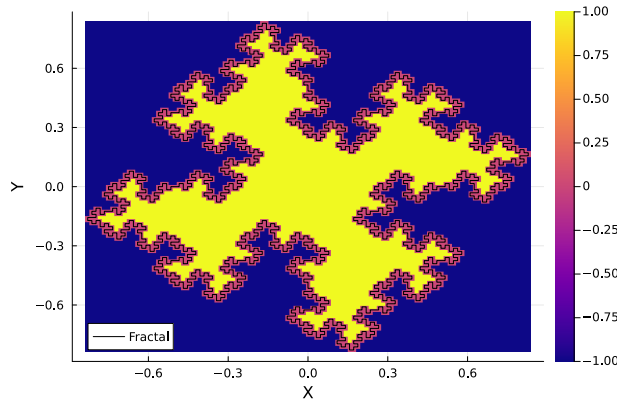

(a) Winding number

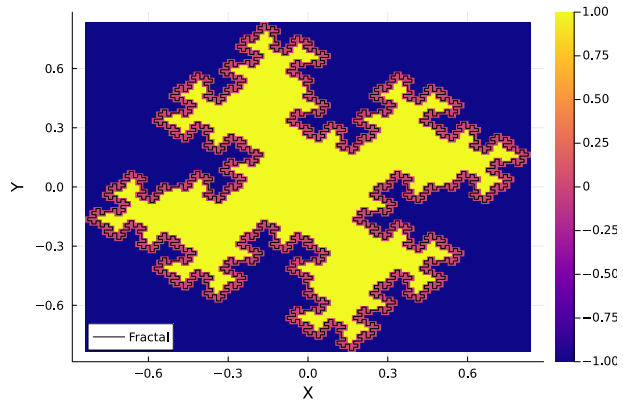

(b) Within

FIG. 2: The methods used to find the points inside the fractal, here for fractal level $l = 3$. Value of points outside are set to -1, points on the border 0 and points inside $+1$.

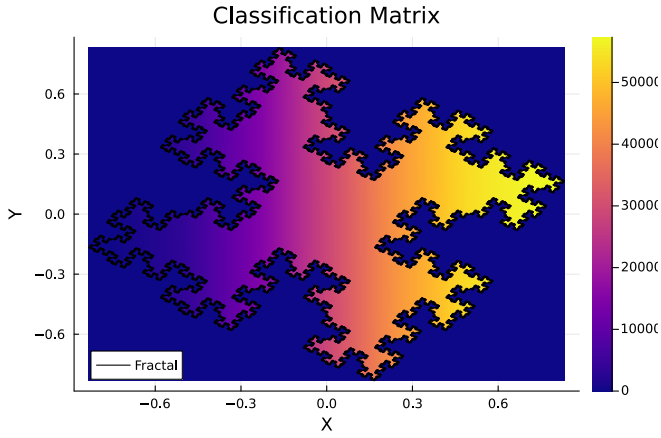

FIG. 3: Classified lattice based on fractal, with labeling of points within fractal. Here $l = 4$.

TABLE II: Eigenvalues and related quantities using a fourth-order finite difference stencil.

mode_index	eigenvalue	degeneracy	ratio	N_w	dN_w
0	9.44438	1	2.12573	0.0	7.09801
1	14.1809	2	3.19182	1.0	15.0028
2	14.1809	2	3.19182	2.0	14.0028
3	14.4561	1	3.25377	3.0	13.63
4	14.532	1	3.27086	4.0	12.8052
5	15.1075	2	3.40039	5.0	13.1625
6	15.1075	2	3.40039	6.0	12.1625
7	17.6885	1	3.98132	7.0	17.8985
8	18.9501	1	4.26527	8.0	20.5768
9	19.4969	2	4.38835	9.0	21.2498

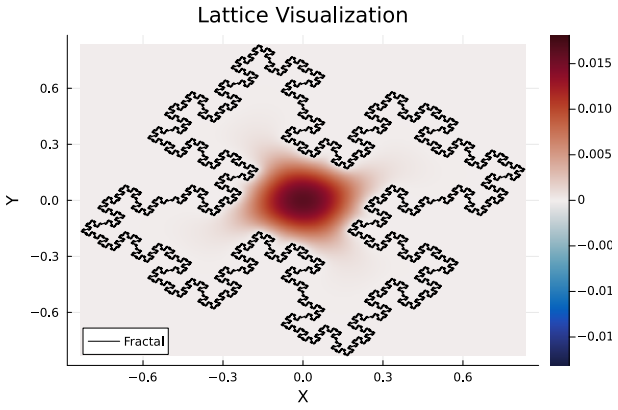

(a) Mode 0

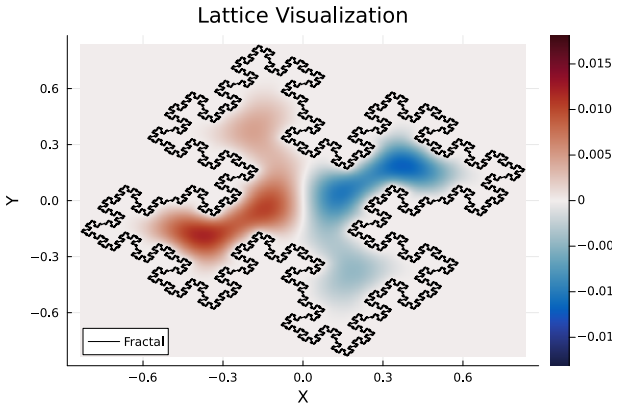

(b) Mode 1

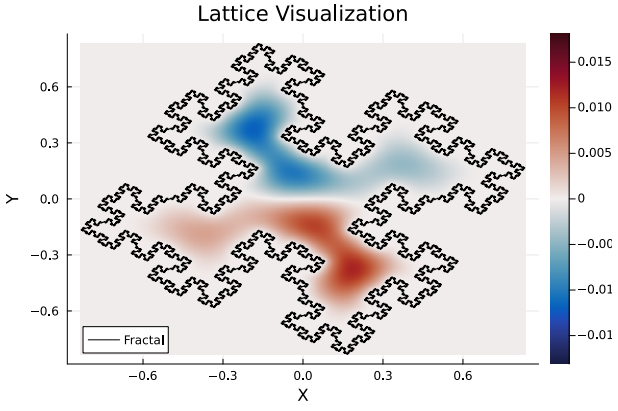

(c) Mode 2

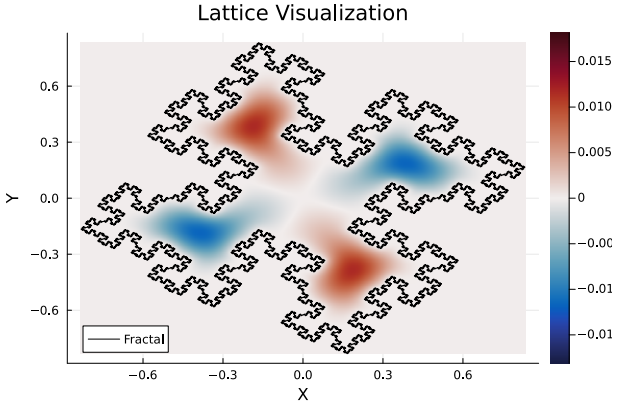

(d) Mode 3

FIG. 4: Three smallest modes

.

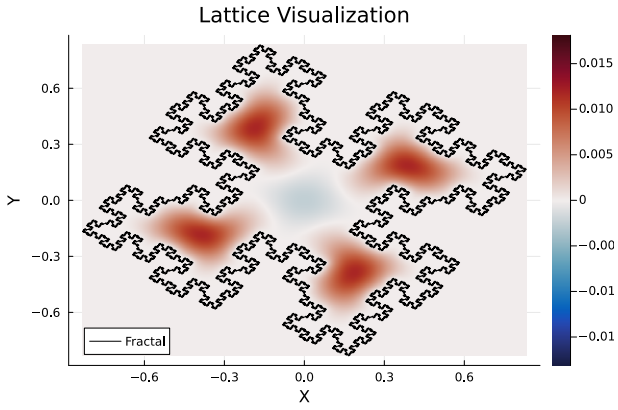

(a) Mode 4

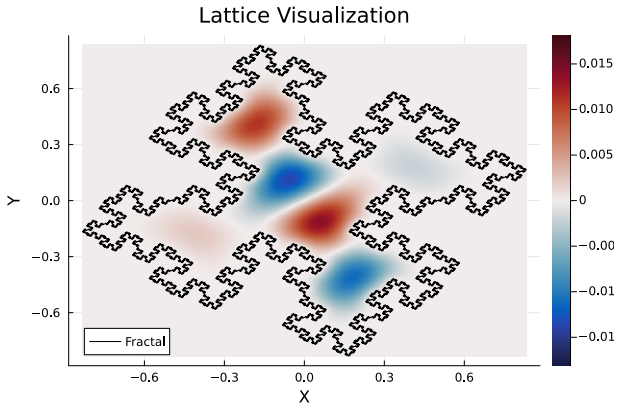

(b) Mode 5

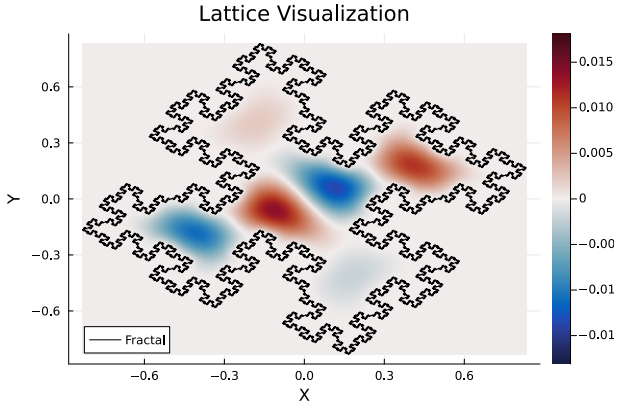

(c) Mode 6

FIG. 5: Modes 4 to 6

.

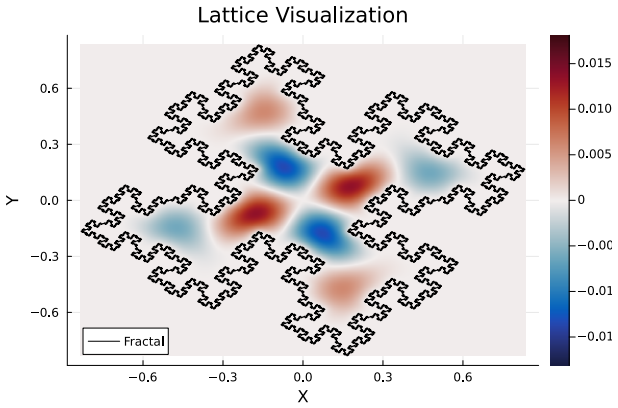

(a) Mode 7

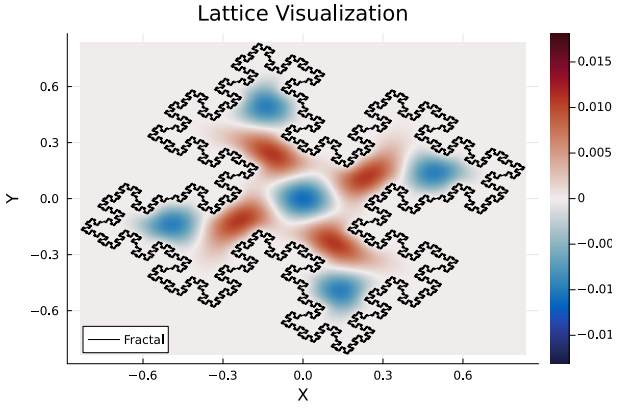

(b) Mode 8

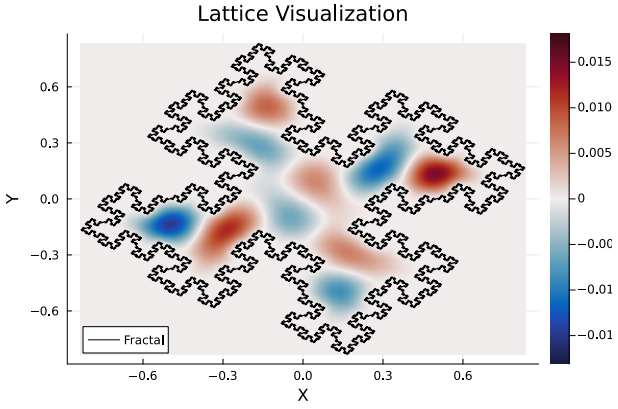

(c) Mode 9

FIG. 6: Eigenmodes 7 to 10

REFERENCES

[1]V. Simonsen, N. Hale, and I. Simonsen, "Eigenmodes of fractal drums: A numerical student experiment," American Journal of Physics **92** (2024), https://doi.org/10.48550/arXiv.2309.13613.
[2]T. Theoharis, G. Papaioannou, P. Nikolaos, and P. N. M., *Graphics and Visualization* (A K Peters, 2021).
[3]R. H. P. J. C. Tannehill, D. A. Anderson, *Computational FLuid Mechanics and Heat Transfer Second edition* (Taylor and Francis, 1997).

V. APPENDIX A: